DISCUSSION

INTRODUCTION

Studies of neovolcanic zones along mid-ocean ridges have left many uncertainties about volcanic–tectonic relations at spreading centers unresolved. To better understand these relations, the median valley of Mohns Ridge in the Norwegian–Greenland Sea (fig. 1) was investigated in August 1987 aboard the RV *Knorr* using the SeaMARC 1B sidescan-sonar system and the Argo photographic–video system. Mohns Ridge is a site of active sea-floor spreading between the North American plate and the Eurasian plate. The sidescan-sonar imagery with generalized bathymetry, selected Argo images, and interpretive geologic maps derived from these images are presented in this report.

The strategy used during this investigation was to survey in detail a few small areas of recent volcanism. Because of a lack of reconnaissance data, the selection of study areas was based on small-scale bathymetic hypotheses developed from the current understanding of mid-ocean ridge processes. Studies of mid-ocean ridges have suggested that the elevation of the ridge axis reflects the height reached by upwelling magma from place to place along the axis, a height that is controlled by the magma budget (Francheteau and Ballard, 1983; Macdonald and others, 1984; Detrick and others, 1987). Topographic highs along the ridge axis are thought to reflect points of magmatic upwelling: they typically display abundant volcanic sheet flows or fluid lava, they lack fissures and faults, and they are sites of active hydrothermal processes (Lonsdale, 1977; Ballard and Francheteau, 1982; Macdonald, 1982; ARGO–RISE Group, 1988). Away from the axial topographic high, volcanic activity should decrease. Therefore, the principal areas we chose for study (fig. 2) were, first, the flank of a topographic high within the median rift valley (Area 1) and, second, the crest of a topographic high within the valley (Area 2). An area 47 km north of the Jan Mayen Fracture Zone (fig. 2, Area 3) was also investigated, but was abandoned because reconnaissance showed that this area was completely covered by bioturbated, rippled sediment. Although evidence of recent volcanic activity (fresh, glassy basalt that has minimal sediment cover) was not observed in Areas 1 and 2, both tectonic and volcanic trends were apparent in the data, thus allowing comparison.

TECTONIC SETTING

Mohns Ridge extends northeastward from the Jan Mayen Fracture Zone to the Greenland Fracture Zone and separates the Greenland Basin to the northwest from the Lofoten Basin to the southeast (fig. 1). The median valley in the study areas is about 45 km wide and from 400 to 1,400 m deep (fig. 2). Its trend of N. 60° E. is oblique to the inferred lithospheric spreading direction of N. 60° W. (Minster and Jordan, 1978). The spreading rate along Mohns Ridge is slow, about 1.6 cm/yr, and there is a 2 to 14 percent asymmetry in spreading half-rates for 0 to 90 m.y. B.P. (the rate is somewhat faster on the Eurasian-plate flank of the ridge; Vogt and others, 1982). The spreading-rate asymmetry decreases to the northeast and has been attributed to a tendency for the obliquely spreading ridge axis to reorient itself counterclockwise to reduce the obliqueness (Vogt and others, 1982).

METHODS

Assessment of the sea-floor topography and distribution of rock types along the median valley of Mohns Ridge was determined from about 200 km of Argo video, 560 km of 12-kHz echo-sounder profiles, and 335 km^2 of SeaMARC 1B imagery. SeaMARC 1B is a deeply towed (400 to 600 m above the sea floor) sidescan-sonar system that generates rectilinear plan-view acoustic images of the sea floor in swaths as much as 5 km wide (Chayes, 1983). The acoustic sensors of SeaMARC 1B consist of sidescan transducers (27 kHz to port and 30 kHz to starboard with a 1.7° horizontal beam) and a 4.5-kHz subbottom profiler. A part of the SeaMARC data-acquisition system failed during the cruise; as a result, 1,250 m of the near-range imagery on the port channel and 1,250 m of the far-range imagery on the starboard channel were lost (50 percent of the total swath width), thus precluding construction of sidescan-sonar mosaics. Presented here is the recovered sidescan-sonar imagery with bathymetric overlays on maps A, C, and E, and the imagery with interpretive geologic overlays on maps B, D, and F. Lighter tones on the sidescan-sonar imagery indicate areas of sea floor that have relatively low acoustic backscattering intensity, whereas darker tones indicate areas of higher backscattering intensity. The SeaMARC data were processed by computer using techniques modified from Chavez (1986) and Malinverno and others (1990). Seismic-reflection profiles acquired with the SeaMARC 4.5-kHz profiler were generally of poor quality and had negligible subbottom penetration.

Argo is a deeply towed photographic–video system that operates at heights of 10 to 40 m above the sea floor (Harris and Ballard, 1986; Harris and others, 1987). The Argo sled carries three silicon-intensified target video cameras, one having a 12-mm down-looking lens, one a 24-mm forward-looking lens, and one a 24- to 80-mm down-looking zoom lens. The sled also carries a 35-mm still camera that is capable of collecting 800 high-resolution color photographs per deployment, a high-resolution charge-coupled electronic still camera (ESC), and a thermistor capable of detecting temperature fluctuations of 0.1°C. Argo was towed at an altitude of 12 m above the sea floor for most of the investigation, which provided a real-time high-resolution view of the sea floor in approximately 8-m swaths.

Navigation of the Argo and SeaMARC systems was performed by integrating Loran-C, Global Positioning System, and transit-satellite positional data. A long-baseline bottom transponder system was included in the navigation of Argo while conducting a detailed survey of a segment of Area 1 (fig. 3). Positioning accuracy was approximately 300 m for the general SeaMARC and Argo surveys and about 5 m for the detailed survey.

VOLCANIC UNITS

The observed basaltic lava was classified morphologically as (1) sheet flows, including smooth, ropy, and hackly varieties (figs. 4*A*–*C*); (2) pillow basalt (fig. 4*D*), and (3) rubble (fig. 4*E*). The volcanic terranes were masked by pelagic sediments that ranged from a mere dusting of sediments to complete coverage. Currently, there is no accurate method for directly dating young mid-ocean ridge basalts. The appearance of the basalt luster and the percentage of sediment cover can be used to estimate the relative age of the basalt (van Andel and Ballard, 1979; Ballard and others, 1981, 1982; ARGO–RISE Group, 1988; Uchupi and others, 1988). Glassy luster indicates fresh basalt, whereas dull luster indicates older material. The sedimentation rate in the study areas is approximately 1 to 2 cm/100 yrs (Thiede and others, 1986). Thus, volcanic rocks having negligible sediment cover may be less than 500 years old; however, this estimate may be skewed by such factors as variable topographic relief and redistribution of sediment by bottom currents.

The amount of sediment cover in each study area suggests that none of them were volcanically active at the time of the survey; that is, fresh glassy basalt having minimal sediment cover was not observed. No hydrothermal activity was directly observed in any of the three study areas, although evidence of hydrothermal activity in Areas 1 and 2 includes temperature anomalies, sediment of apparent hydrothermal origin, and sediment elutriation structures (blowouts). In Area 1, a density plume in the water column was also observed.

SEA-FLOOR OBSERVATIONS

Area 1

Area 1 is located within the median valley of Mohns Ridge between longitudes 1°05′ W. and 0°05′ E. (fig. 2). The floor of the median rift valley is characterized by a rugged topography of irregularly shaped volcanic edifices. The SeaMARC imagery (maps A and C) depicts a complex pattern of backscatter intensity. Volcanic edifices produce mottled high backscatter, whereas areas of heavy sediment cover (and acoustic shadows) produce low backscatter. A ridge about 5 km wide, 500 m high, and at least 15 km long trends approximately N. 55° E. across the southwest segment of Area 1 (maps A and B). Bathymetric details are not clear because the bathymetry is based solely on profiles collected along the SeaMARC and Argo tracklines.

Also shown on the SeaMARC imagery are lineaments expressed at the sea floor. These lineaments display a wide azimuth-frequency distribution (maps B and D). The major modal trend of the lineaments is between N. 50° E. and N. 54° E. (fig. 5, 50°–54°), and a minor modal trend is between N. 90° E. and N. 86° W. (fig. 5, 90°–94°). The number of lineaments per unit area of sea floor increases toward the northeast in Area 1 (maps B and D), along with an increase in the water depth (maps A and C).

Lineaments are interpreted to be, for the most part, fault scarps (interpretation from the Argo data). Scarps as much as 175 m high, some with vertical faces (fig. 6*A*) were observed by the Argo system throughout Area 1. The scarps are too numerous to plot all of them on maps B and D and on figure 3, and most were too small (~20 m) to be resolved by the SeaMARC system. With few exceptions, the large scarps imaged with SeaMARC appear to be tectonic features (fault scarps) while many of the smaller scarps and the volcanic ridge in the central part of Area 1 are indicative of constructional volcanism (scarps having lava draperies). The scarps and slopes of the volcanic edifices were typically associated with fields of volcanic rubble composed of broken pillow basalt (fig. 6*B*) or with chutes of sediment/rubble debris-flow deposits (fig. 6*C*).

The most extensive volcanic rock unit observed in the southwest segment of Area 1 is pillow basalt (map B and fig. 3). These pillow basalts have a dull luster and various amounts of sediment cover (dusting to 100 percent cover) and rubble. The dull appearance and different percentages of sediment cover indicate that the pillow basalts are of mixed age and are not fresh extrusions.

The northeast-trending volcanic ridge in the central part of Area 1 is composed primarily of pillow basalts (map B). Argo data show that these pillow basalt flows are of varied age: sediment cover ranges from 0 to 100 percent and luster ranges from dull to very dull. At the southwest limit of the ridge, sheet flows (in some places intermixed with older pillow basalts) were observed, which suggests that this area of the ridge had the most recent volcanic activity (following the findings of Lonsdale, 1977; Ballard and Francheteau, 1982; Macdonald, 1982; ARGO–RISE Group, 1988).

There are a number of indications that the southwest segment of Area 1 is an area of hydrothermal activity. These indications include minor increases in water temperature, the presence of large colonies of sponges, and sediment that appears to be hydrothermal in origin based on its yellow color and punky appearance (figs. 6*D* and *E*). These suspected hydrothermal sediments are often associated with relatively fresh appearing pillow basalts (fig. 6*F*) or sheet flows. In addition, a feature interpreted as a density plume in the water column was recorded on the SeaMARC 4.5-kHz-subbottom profiler (fig. 7), although a detailed search of the area (fig. 3) using Argo imagery did not reveal the source. A series of features interpreted to be sediment elutriation structures or blowouts (fig. 6*G*) were recorded on the Argo images (map B and fig. 3). The blowouts were found in areas with nearly 100 percent sediment cover. In these areas, fissures in the underlying bedrock are exposed at the floor of linear depressions in the sediment. We propose that these linear depressions were caused by hydrothermal fluid emanating from the bedrock fissures at a flow velocity sufficient to either blow overlying sediment away from the fissures, or to retard sediment accumulation along the fissures. In some cases, the removed sediment was observed covering adjacent bioturbated sediment, which suggests recent activity.

Area 2

Area 2 is located on an axial topographic high within the median valley of Mohns Ridge between longitudes 3°40′W. and 3°00′W. (fig. 2; Vogt and others, 1982). The floor of the median valley is characterized by a rugged topography of volcanic edifices, similar to Area 1. Three ridges about 4 km wide, 600 m high, and 11 km long trend approximately N. 50° E. to N. 60° E. across Area 2 (maps E and F).

The SeaMARC imagery (map E) depicts a pattern of backscatter intensity similar to that of Area 1, with high-backscatter intensity from the volcanic edifices and low backscatter from areas of heavy sediment cover (and acoustic shadows). Lineaments interpreted to be fault scarps are also shown on the SeaMARC imagery of Area 2 (map F), but they are not as numerous per unit area of sea floor as in Area 1 (maps B and D). The lineaments display a wide range of trends (fig. 8) with a major modal trend between N. 55° E. and N. 59° E. (55°–59°) and minor trends between N. 80° W. and N. 76° W. (100°–104°) and N. 70° W. and N. 66° W. (110°–114°).

Scarps similar to those encountered in Area 1 were viewed using Argo in Area 2 (fig. 9*A*). Again, most of these scarps were too small to be resolved with SeaMARC. Most of the large scarps appear to be tectonic features, while many of the smaller scarps are indicative of constructional volcanism. Again, the scarps and slopes of the volcanic ridges were associated with fields of volcanic rubble (fig. 9*B*) or with chutes of sediment/rubble debris-flow deposits (fig. 9*C*).

Argo data show that the most extensive volcanic rock unit in Area 2 is pillow basalt that has a dull luster and various percentages of sediment cover (map F), which indicates relatively old flows.

Two of the three ridges in Area 2 were investigated using Argo. These ridges are composed of pillow basalts of various ages. A field of sheet flows was traversed along the southwestern terminus of the most southerly ridge (figs. 9*D* and *E*), which is relatively flat topped and resembles a subaerial tuya (map E). These sheet flows are dull in appearance, are covered with minor amounts of sediment, and typically are intermixed with relatively fresh pillow basalt. The general lack of lineaments (faults) on the SeaMARC imagery (map F), the occurrence of sheet flows and pillow basalts that have minimal sediment cover (figs. 9*F* and *G*), a minor temperature anomaly, and sediment blowouts (fig. 9*H*) suggest that the southernmost ridge is the site of the most recent volcanism found during this investigation.

DISCUSSION AND CONCLUSIONS

Mohns Ridge is an area of sea-floor spreading and associated volcanic activity. As with other mid-ocean-ridge systems, recent volcanic activity along Mohns Ridge is discontinuous, both temporally and spatially. Sea-floor observations in the study areas indicate that they were not volcanically active at the time of the survey. Until an accurate technique of dating relatively young mid-ocean ridge basalts is developed, the relative age of volcanic units can be only qualitatively estimated on the basis of the general appearance of the rock outcrops and the amount of sediment cover. The differences in sediment cover and appearance of the basalt suggest varied ages for the lava units, including those that compose individual linear volcanic ridges. Hydrothermal activity is indicated in Area 1 on the basis of a density plume, a limited area of hydrothermal sediments, minor temperature anomalies, and the occurrence of large colonies of sponges (fig. 3, lat 71°56′40″N., long 0°47′45″W.). A temperature anomaly and the occurrence of sediment blowouts on the southernmost linear volcanic ridge in Area 2 also indicate possible hydrothermal activity.

Francheteau and Ballard (1983) predicted that a topographic high above the crest of a magma reservoir should be mantled by sheet flows and have thermal effects at a maximum. Away from the high, volcanic activity should decrease. Active volcanism tends to mask tectonic features such as fault scarps and rubble aprons. It follows that sea-floor terrain with a small number of fault scarps is an area of high volcanic activity. In Area 1, the number of faults increases toward the northeast, away from the axial topographic high, and, in general, the terrain displays the features outlined by Francheteau and Ballard (1983) and observed on other mid-ocean ridge segments that indicate the elevation of the ridge axis is a direct measure of the magma budget (Macdonald and others, 1984; Detrick and others, 1987; ARGO–RISE Group, 1988; Uchupi and others, 1988). Similarly, Area 2, the crest of an axial topographic high, contains fewer faults per unit area of sea floor than Area 1, which suggests greater volcanic activity. Note also that the two southernmost linear volcanic ridges in Area 2 are relatively undisturbed by faulting. The lack of faulting along with the extensive sheet flows and relatively young pillow basalts located on the southernmost ridge suggests that this area shows the most recent volcanic activity found in this investigation.

The systems of ridges located in Areas 1 and 2 are composed of various morphological types of lava of different ages, which is similar to the polygenetic volcanoes found on Rekjanes Ridge (Johnson and Jakobsson, 1985). These ridges and the irregularly shaped volcanic edifices are separated from one another by sediment-covered depressions. Both the orientation of the linear volcanic ridges and the major trend of inferred faults (lineaments on the SeaMARC imagery) are roughly parallel to the trend of the ridge axis (figs. 11 and 12). We propose that the linear volcanic ridges are elementary spreading cells in an obliquely spreading system; that is, the dominant ~N. 60° E.-trending fault system forms the principal conduit for magma to reach the sea floor, thus forming the linear volcanic ridges. The secondary fault trends (figs. 5, 8, 11, and 12) found in the study areas are oblique to the lithospheric spreading direction (parallel to the strike of the Jan Mayen Fracture Zone) and to the obliquely spreading ridge axis; these trends are puzzling, but they must have a strong component of strike-slip motion.

Trends of the volcanic and tectonic features found during this investigation are not consistent with the findings of Renard and others (1989) who studied the sea-floor topography along a segment of Mohns Ridge centered near lat 72°20′N., long 1°30′E. by using a variety of geophysical systems, which included a Hydrosweep swath bathymetry system. Renard and others (1989) reported an en echelon pattern of volcanic ridges (described as polygenetic volcanoes) within the median rift valley oriented N. 30° E. (030°), oblique to the strike of the ridge axis but perpendicular to the lithospheric spreading direction. Renard and others (1989) concluded that the term "oblique spreading" is inappropriate when used to describe the tectonic setting of Mohns Ridge and that these en echelon volcanic ridges are elementary spreading cells. In Areas 1 and 2 of the present investigation, no volcanic or tectonic trends were found that parallel the en echelon pattern of volcanic ridges as described by Renard and others (1989) (fig. 10). In fact, the linear volcanic ridges in Areas 1 and 2 are oriented oblique to the lithospheric spreading direction and parallel to the trend of Mohns Ridge. Therefore, we would suggest that oblique spreading is applicable to the description of the tectonics of this segment of Mohns Ridge.

The conflicting interpretations of the tectonic processes affecting Mohns Ridge may merely be symptomatic of a general lack of high-quality reconnaissance data. Results from an extensive geophysical survey along an 800-km length of the Mid-Atlantic Ridge between the Kane and Atlantis Fracture Zones, an area of sea-floor spreading, showed that the style of tectonic extension varies markedly along the ridge (Sempere and others, 1990). Variation in spreading rates has also been shown to result in dramatic along-axis changes in median-valley morphology and style of faulting (Karson and others, 1987). Thus, prior to conducting further detailed or high-resolution studies of Mohns Ridge, both multi-beam bathymetric and wide-swath sidescan-sonar surveys should be completed over the entire system. Only then will it be possible to integrate seemingly conflicting results of the higher resolution investigations into a regional tectonic model.

ACKNOWLEDGEMENTS

We thank Captain Bowen and the crew of the RV *Knorr* for their cooperation. Robert Ballard, Kurt Smrcina, Stewart Harris, Richard Gallota, and Jefferey Hoy helped develop and coordinate this cruise, which was a portion of a cooperative program between B.D.M. Corporation, McLean Va.; Marine Imaging Systems, Pocasset, Ma.; Woods Hole Oceanographic Institution; the Office of Naval Research; and the U.S. Geological Survey. William Lange provided additional support in processing and presenting the Argo video and photographic data, and Doom Squires provided real-time editing of the ESC data. Special thanks goes to the operations group of the Deep Submergence Laboratory, Woods Hole Oceanographic Institution led by Thomas Dettweiler, without whose help this cruise would not have been possible. William Dillon and Dennis O'Leary provided helpful technical reviews of the final report. Jefferey Zwinakis and Dann Blackwood prepared all the illustrations.

REFERENCES CITED

ARGO–RISE Group, 1988, Geological mapping of the East Pacific Rise axis (10°19′–11°53′N) using the Argo and ANGUS imaging systems: Canadian Mineralogist, v. 26, no 3, p. 467–486.

Ballard, R.D., and Francheteau, Jean, 1982, The relationship between active sulfide deposition and axial processes of the mid-ocean ridge: Marine Technology Society Journal, v. 16, no. 1, p. 8–22.

Ballard, R.D., Francheteau, Jean, Juteau, T.A., Rangin, C.V., and Normark, W.R., 1981, East Pacific Rise at 21°N: The volcanic, tectonic, and hydrothermal processes of the central axis: Earth and Planetary Science Letters, v. 55, no. 1, p. 1–10.

Ballard, R.D., van Andel, T.H., and Holcomb, R.T., 1982, The Galapagos rift zone at 86°W, Part 5: Variations in volcanism, structure, and hydrothermal activity along a 30-kilometer segment of the rift valley: Journal of Geophysical Research, v. 87, no. B2, p. 1149–1161.

Chavez, P.S., 1986, Processing techniques for digital sonar images from GLORIA: Photogrammetric Engineering and Remote Sensing, v. 52, no. 3, p. 1133–1145.

Chayes, D.N., 1983, Evolution of SeaMARC 1, *in* Third working symposium on oceanographic data systems, Proceedings: Institute of Electronics and Electrical Engineers Computer Society Press, p. 103–108.

Detrick, R.S., Buhl, P.O., Vera, E.A., Mutter, J.S., Orcutt, J.R., Madsen, J.O., and Brocher, Thomas, 1987, Multichannel seismic images of an axial magma chamber along the East Pacific Rise between 9° and 13°N.: Nature, v. 326, no. 6108, p. 35–41.

Francheteau, Jean, and Ballard, R.D., 1983, The East Pacific Rise near 21°N, 13°N, and 20°S: Inferences for along-strike variability of axial processes of the mid-ocean ridge: Earth and Planetary Science Letters, v. 64, no. 1, p. 93–116.

Harris, S.E., and Ballard, R.D., 1986, ARGO: Capabilities for deep ocean exploration, *in* v. 1 *of* Oceans '86, Conference Record: Washington, D.C., Marine Technology Society and Institute of Electronics and Electrical Engineers, p. 6–12.

Harris, S.E., Squires, R.H., and Bergeron, E.M., 1987, Underwater imagery using an electronic still camera, *in* v. 3 *of* Oceans '87, Proceedings: Washington, D.C., Marine Technology Society and Institute of Electronics and Electrical Engineers, Ocean Engineering Society, v. 3, p. 1242–1245.

Johnson, G.L., and Jakobsson, S.P., 1985, Structure and petrology of the Reykjanes Ridge between 62°55′N and 63°48′N: Journal of Geophysical Research, v. 90, no. B12, p. 10,073–10,083.

Karson, J.A., Thompson, Geoffrey, Humphris, S.E., Edmond, J.M., Bryan, W.B., Brown, J.R., Winters, A.T., Pockalny, R.A., Casey, J.F., Campbell, A.C., Klinkhammer, G.B., Palmer, M.R., Kinzler, R.J., and Sulanowska, M.M., 1987, Along-axis variations in seafloor spreading in the MARK area: Nature, v. 328, no. 6132, p. 681–685.

Lonsdale, Peter, 1977, Structural geomorphology of a fast-spreading rise crest: The East Pacific Rise near 3°25′S.: Marine Geophysical Research, v. 3, no. 3, p. 251–243.

Macdonald, K.C., 1982, Mid-ocean ridges: Fine scale tectonic, volcanic, and hydrothermal processes within the plate boundary zone: Annual Review of Earth and Planetary Sciences, v. 10, p. 155–190.

Macdonald, K.C., Sempere, J.C., and Fox, P.J., 1984, East Pacific Rise from Siqueiros to Orozco Fracture Zones: Along-strike continuity of the axial neovolcanic zone and structure and evolution of overlapping spreading centers: Journal of Geophysical Research, v. 89, no. B7, p. 6049–6069.

Malinverno, Alberto, Edwards, Margo, and Ryan, W.B.F., 1990, Processing of SeaMARC swath sonar data: Institute of Electronics and Electrical Engineers Journal of Oceanic Engineering, v. 15, no. 1, p. 14–23.

Minster, R.B., and Jordan, T.H., 1978, Present-day plate motions: Journal of Geophysical Research, v. 83, no. B11, p. 5331–5354.

Renard, V., Avedik, F., and Geli, L., 1989, Mohns Ridge, Norwegian–Greenland Sea: Morphology and structure near 72°N [abs.]: International Geological Congress, 28th, Abstracts, v. 2, p. 687–688.

Schwab, W.C., Holcomb, R.T., and van Dover, C.L., 1988, Preliminary presentation and interpretation of ARGO/SeaMARC 1B reconnaissance investigation of Mohns Ridge, Norwegian Sea: U.S. Geological Survey Open-File Report 88–23, 3 sheets, 21 p.

Sempere, J.C., Purdy, G.M., and Schouten, Hans, 1990, Segmentation of the Mid-Atlantic Ridge between 24°N and 30°40′N: Nature, v. 344, no. 6265, p. 427–431.

Thiede, Jorn, Diesen, G.W., Knudsen, B.E., and Snare, T.B., 1986, Patterns of Cenozoic sedimentation in the Norwegian–Greenland Sea: Marine Geology, v. 69, no. 3/4, p. 323–352.

Uchupi, Elazar, Schwab, W.C., Ballard, R.D., Cheminee, J.L., Francheteau, Jean, Hekinian, Roger, Blackman, D.K., and Sigurdsson, Haroldur, 1988, An ANGUS/Argo study of the neovolcanic zone along the East Pacific Rise from the Clipperton Fracture Zone to 12°N: Geo-Marine Letters, v. 8, no. 3, p. 131–138.

van Andel, T.H., and Ballard, R.D., 1979, The Galapagos Rift Zone at 86°W, Part 2: Volcanism, structure, and evolution of the rift valley: Journal of Geophysical Research: v. 84, no. B10 p. 5390–5406.

Vogt, P.R., Kovacs, L.C., Bernero, C.T., and Srivastava, S.P., 1982, Asymmetric geophysical signatures in the Greenland–Norwegian and southern Labrador Seas and the Eurasia Basin: Tectonophysics, v. 89, no. 1–3 p. 95–160.

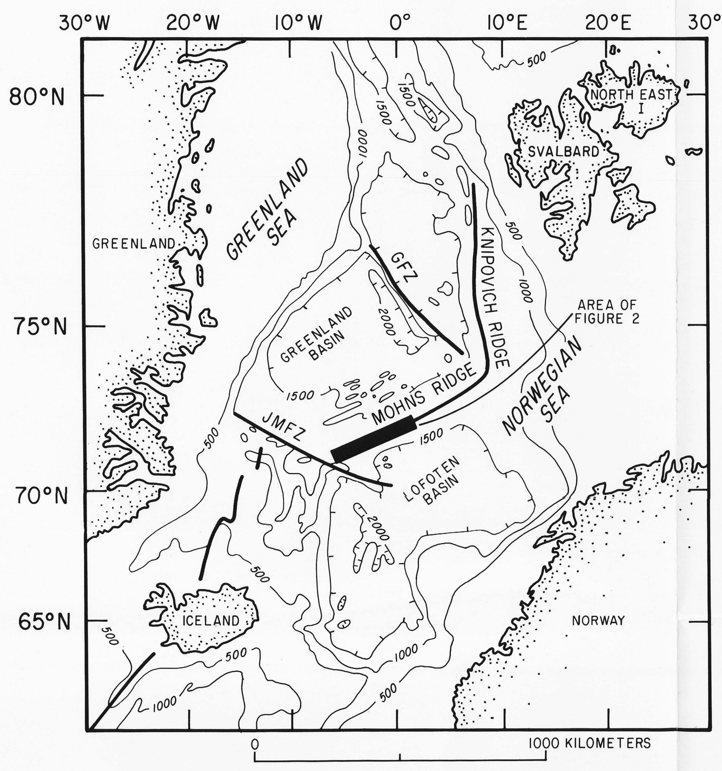

Figure 1.—Location map showing Mohns Ridge, Jan Mayen Fracture Zone (JMFZ), and Greenland Fracture Zone (GFZ). Bathymetry is from Thiede and others (1986). Contour interval is 500 m.

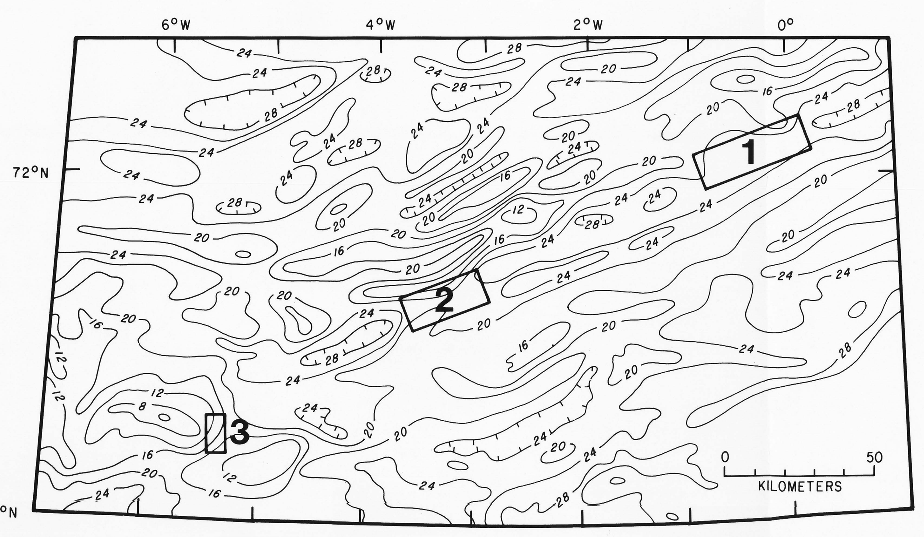

Figure 2.—Location map of the three study areas. Bathymetry was compiled in cooperation with the Office of Naval Operations (Schwab and others, 1988). Contours are in hundreds of meters; contour interval is 400 m.

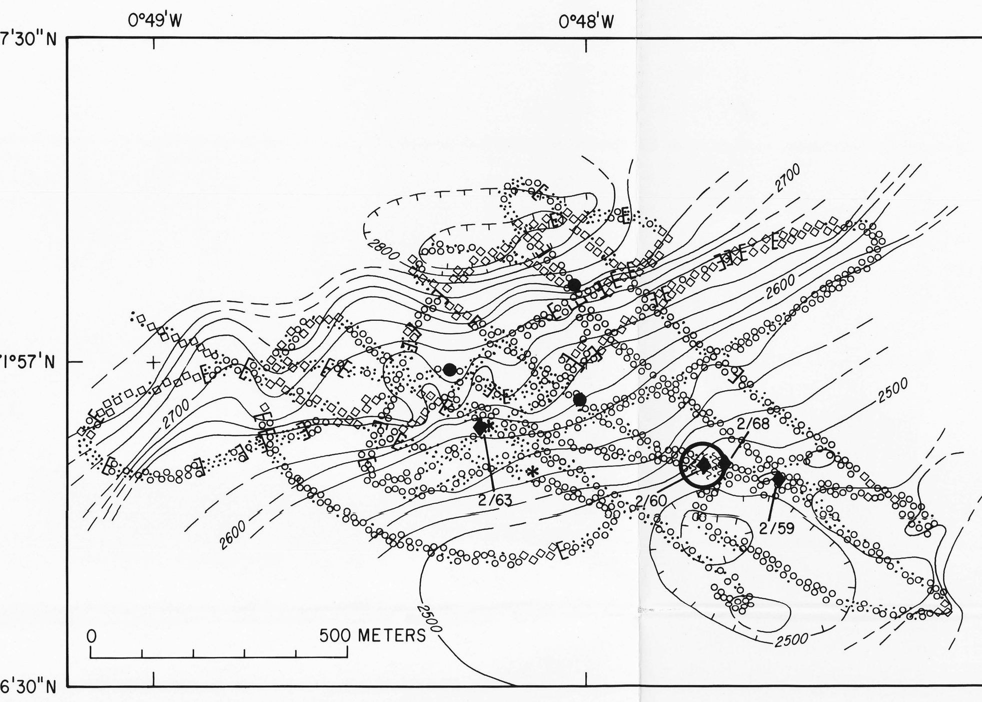

EXPLANATION

Rock types and sediment—Patterns shown only along Argo survey tracklines, where geology was mapped

- Sheet flow—Smooth, hackly, and ropy basalt
- Pillow basalt
- Basalt rubble
- Sediment
- Sediment of probable hydrothermal origin—Shown larger on figure
- Fault scarp—From Argo data. Hachures point downslope
- Sediment blowout
- Temperature anomaly
- Electronic still-camera (ESC) image locatons—Numbers indicate image number
- Bathymetry—Dashed where approximately located. Contour interval is 20 m

Figure 3.—Geologic interpretation and bathymetry of the detailed survey in Area 1. See map B for location. Map pattern of geology based on Argo tracklines.

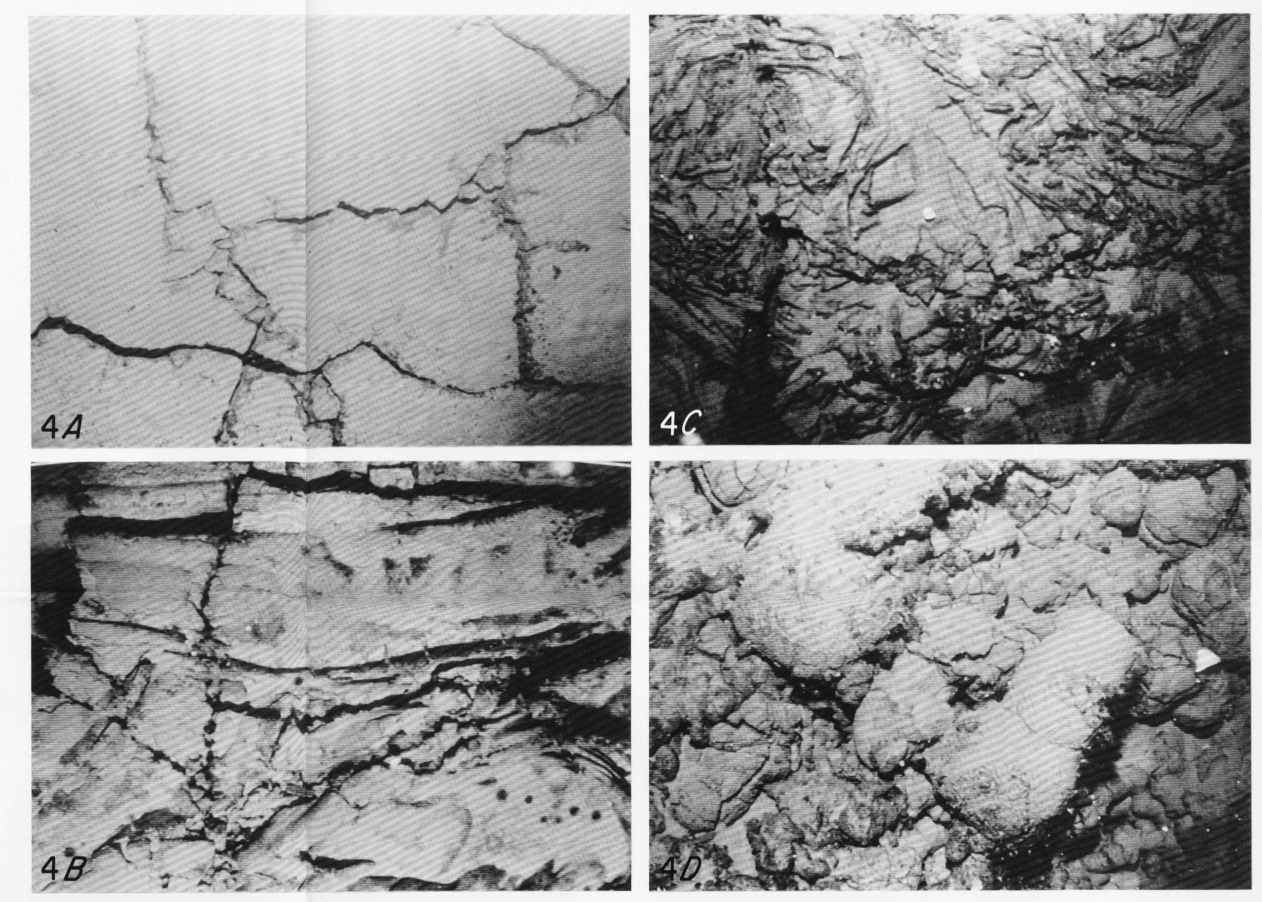

Figure 4.—Electronic still-camera (ESC) images of basalt units. *A*, Smooth sheet flow, ESC image 1/17. *B*, Ropy sheet flow, ESC image 2/31. *C*, Hackly sheet flow, ESC image 1/27. *D*, Pillow basalt, ESC image 1/73. *E*, Volcanic rubble, ESC image 2/11. See map B for image locations. Scale is approximately 4 m across bottom of images.

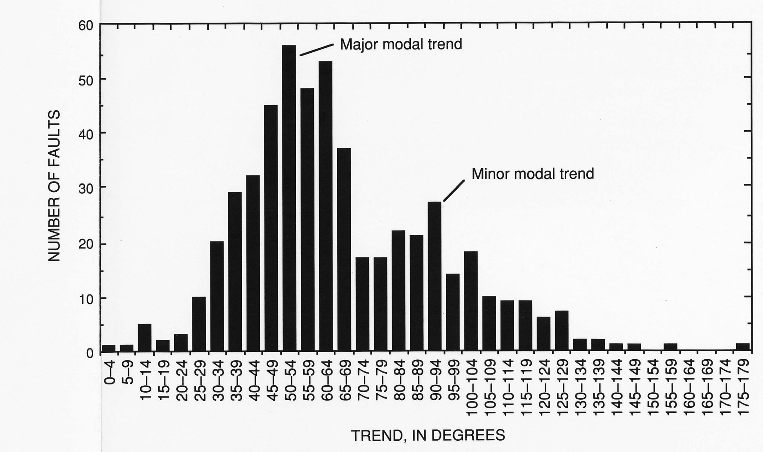

Figure 5.—Trend of lineaments on the SeaMARC 1B imagery in Area 1 (maps B and D).

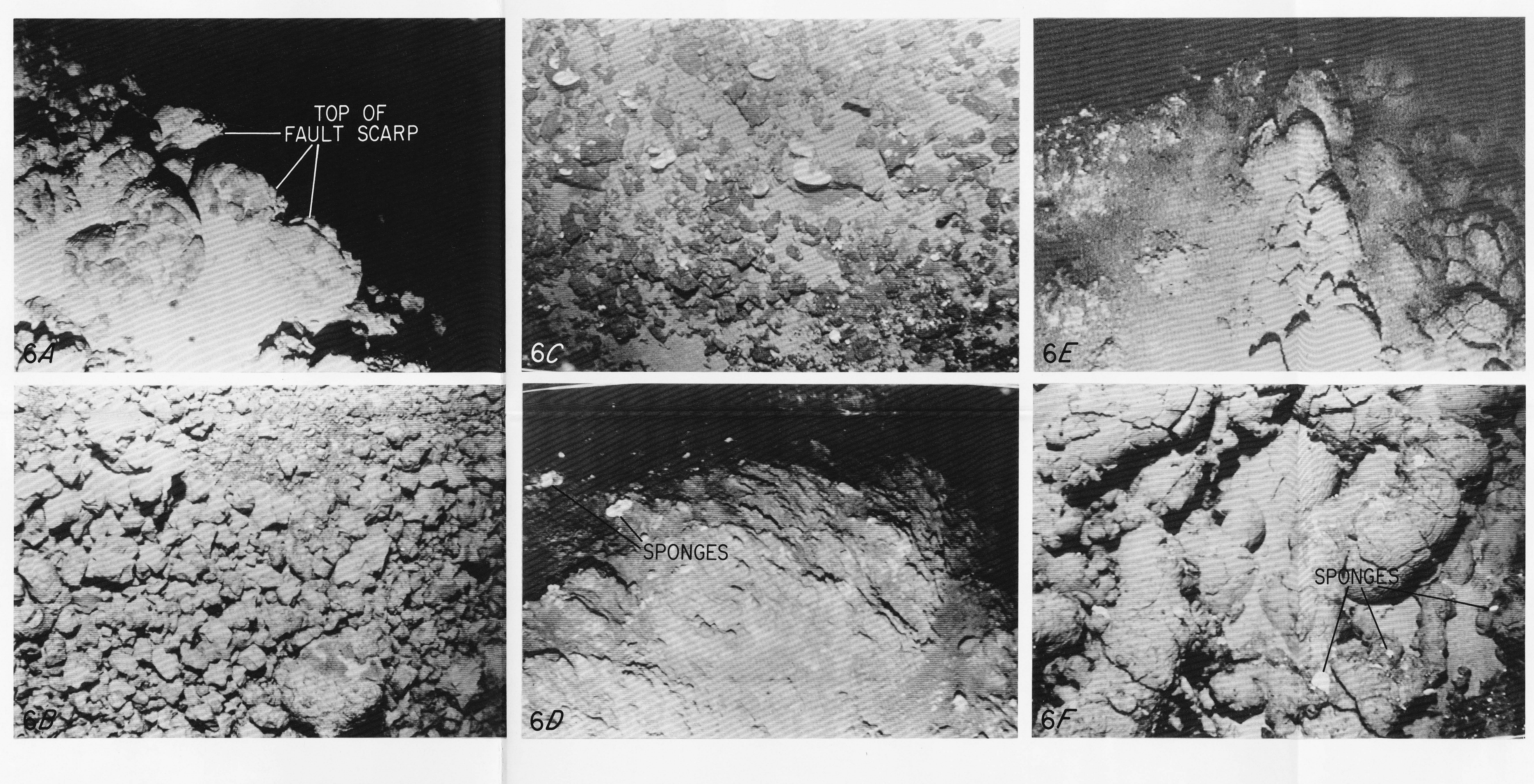

Figure 6.—Selected electronic still-camera (ESC) images collected over Area 1. *A*, Image 1/54 showing top of a fault scarp. *B*, Image 1/75 showing field of rubble at base of a steep slope. *C*, Image 1/49 showing floor of a chute on slope of a volcanic edifice covered by debris-flow (rubble and sediment) deposits and a colony of sponges. *D*, Image 2/60 showing sediment of probable hydrothermal origin. *E*, Image 2/68 showing sediment of probable hydrothermal origin in left half of image in contact with pillow basalt that has substantial sediment cover on right half. *F*, Image 2/59 showing pillow basalt that has relatively minor sediment cover and a few sponges. *G*, Image 2/63 showing a poorly developed sediment blowout and a few sponges (compare to fig. 9*H*). Scale is approximately 4 m across bottom of images. See map B and figure 3 for image locations.

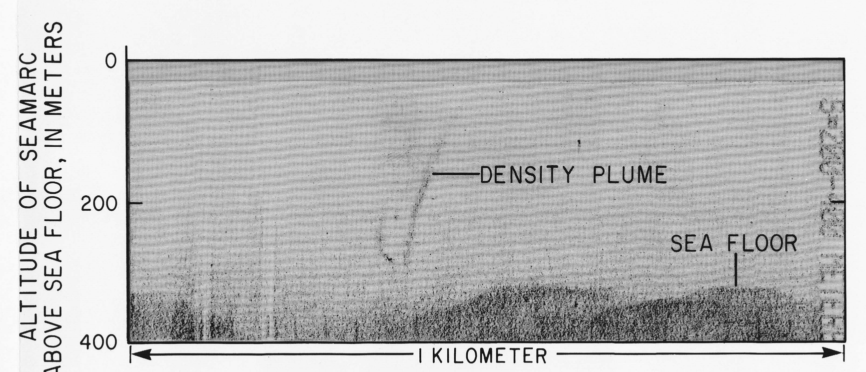

Figure 7.—SeaMARC 4.5-kHz-subbottom profile showing a density plume in the water column. See map B for approximate location.

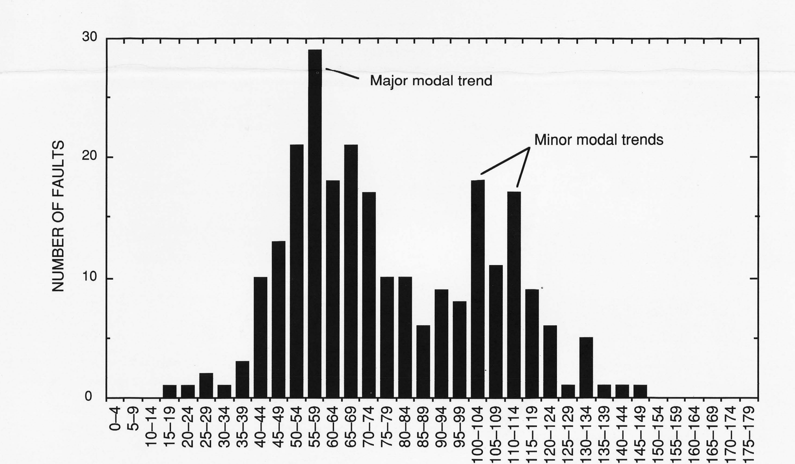

Figure 8.—Trend of lineaments on the SeaMARC 1B imagery in Area 2 (map F).

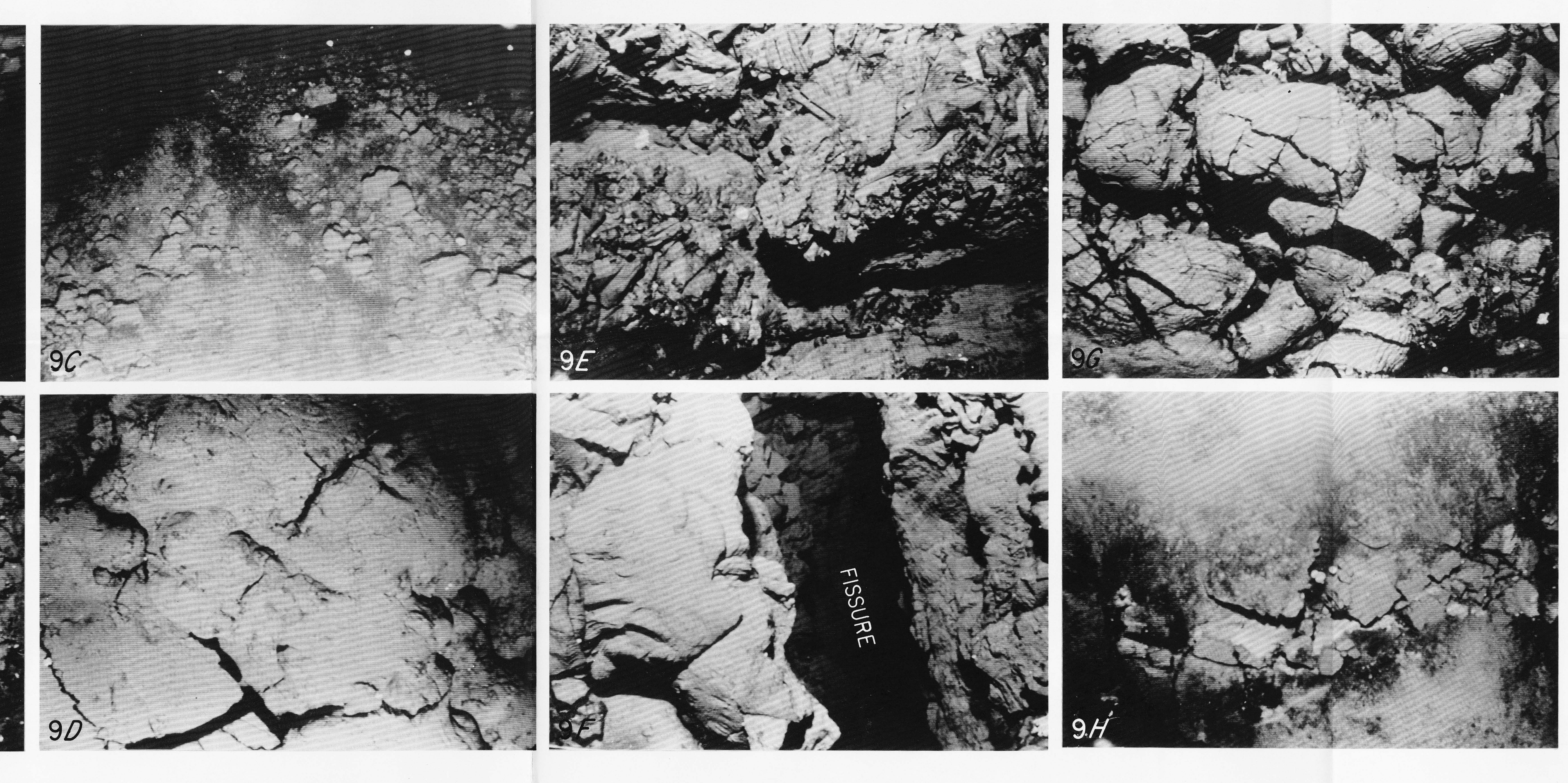

Figure 9.—Selected electronic still-camera (ESC) images collected over Area 2. *A*, Image 4/14 showing top of fault scarp. *B*, Image 3/12 showing field of rubble at base of a scarp. *C*, Image 4/15 showing volcanic slope covered by debris-flow deposits. *D*, Image 4/17 showing smooth sheet flow that has minor dusting of sediment. *E*, Image 3/21 showing hackly sheet flow. *F*, Image 4/2 showing a fissure cutting relatively fresh pillow basalts. *G*, Image 4/13 showing relatively fresh pillow basalts. *H*, Image 3/25 showing a well-developed sediment blowout (center of image). Scale is approximately 4 m across bottom of images. See map F for image locations.

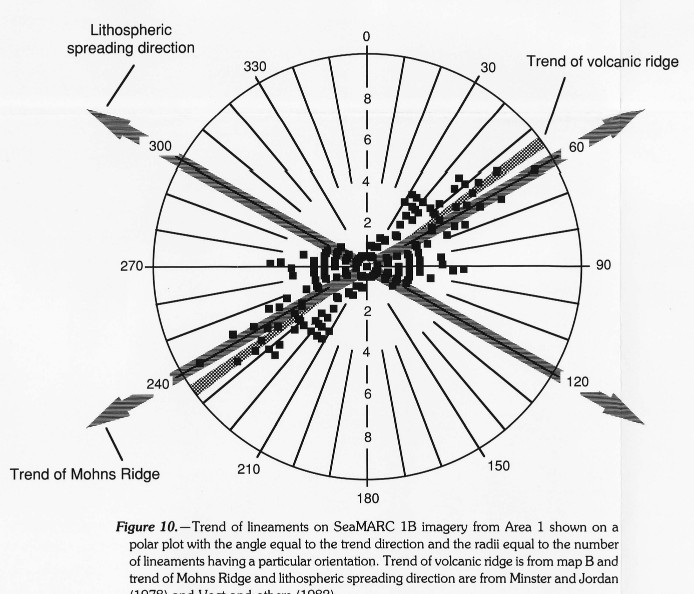

Figure 10.—Trend of lineaments on SeaMARC 1B imagery from Area 1 shown on a polar plot with the angle equal to the trend direction and the radii equal to the number of lineaments having a particular orientation. Trend of volcanic ridge is from map B and trend of Mohns Ridge and lithospheric spreading direction are from Minster and Jordan (1978) and Vogt and others (1982).

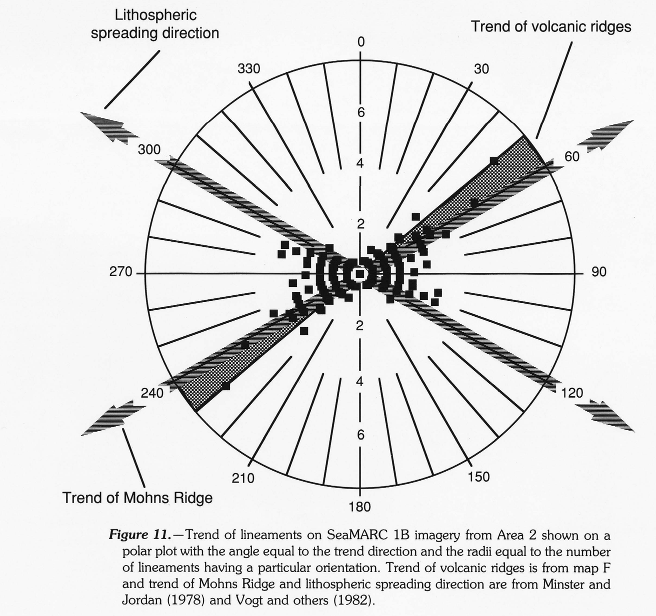

Figure 11.—Trend of lineaments on SeaMARC 1B imagery from Area 2 shown on a polar plot with the angle equal to the trend direction and the radii equal to the number of lineaments having a particular orientation. Trend of volcanic ridges is from map F and trend of Mohns Ridge and lithospheric spreading direction are from Minster and Jordan (1978) and Vogt and others (1982).

GEOLOGIC INTERPRETATION OF SEAMARC 1B AND ARGO IMAGERY IN THE MEDIAN VALLEY OF MOHNS RIDGE, NORWEGIAN–GREENLAND SEA

By
W.C. Schwab[1], Elazar Uchupi[2], R.T. Holcomb[3], and W.W. Danforth[1]

1992

AUTHOR AFFILIATIONS
[1]U.S. Geological Survey, Woods Hole, MA 02543
[2]Woods Hole Oceanographic Institution, Woods Hole, MA 02543
[3]U.S. Geological Survey, Seattle, WA 98195

INTERIOR—GEOLOGICAL SURVEY, RESTON, VA—1992

For sale by U.S. Geological Survey, Map Distribution, Box 25286, Federal Center, Denver, CO 80225